



OPEN ACCESS

EDITED BY

Hesham M. H. Zakaly,
Al-Azhar University, Egypt

REVIEWED BY

A. M. Hassan,
Al-Azhar University, Egypt
Hussam Askar,
Al-Azhar University, Egypt

*CORRESPONDENCE

H. O. Tekin

✉ tekin765@gmail.com

Antoaneta Ene

✉ Antoaneta.Ene@ugal.ro

SPECIALTY SECTION

This article was submitted to
Radiation and Health,
a section of the journal
Frontiers in Public Health

RECEIVED 21 February 2023

ACCEPTED 07 March 2023

PUBLISHED 31 March 2023

CITATION

ALMisned G, Elshami W, Rabaa E, Kilic G, Ilik E,
Sen Baykal D, Ene A and Tekin HO (2023)

Toward the strengthening of radioprotection
during mammography examinations through
transparent glass screens: A benchmarking
between experimental and Monte Carlo
simulation studies.

Front. Public Health 11:1171209.

doi: 10.3389/fpubh.2023.1171209

COPYRIGHT

© 2023 ALMisned, Elshami, Rabaa, Kilic, Ilik,
Sen Baykal, Ene and Tekin. This is an
open-access article distributed under the terms
of the [Creative Commons Attribution License
\(CC BY\)](https://creativecommons.org/licenses/by/4.0/). The use, distribution or reproduction
in other forums is permitted, provided the
original author(s) and the copyright owner(s)
are credited and that the original publication in
this journal is cited, in accordance with
accepted academic practice. No use,
distribution or reproduction is permitted which
does not comply with these terms.

Toward the strengthening of radioprotection during mammography examinations through transparent glass screens: A benchmarking between experimental and Monte Carlo simulation studies

Ghada ALMisned¹, Wiam Elshami², Elaf Rabaa², G. Kilic³, E. Ilik³,
Duygu Sen Baykal⁴, Antoaneta Ene^{5*} and H. O. Tekin^{2,6*}

¹Department of Physics, College of Science, Princess Nourah Bint Abdulrahman University, Riyadh, Saudi Arabia, ²Medical Diagnostic Imaging Department, College of Health Sciences, University of Sharjah, Sharjah, United Arab Emirates, ³Department of Physics, Faculty of Science, Eskisehir Osmangazi University, Eskisehir, Türkiye, ⁴Vocational School of Health Sciences, Medical Imaging Techniques, Istanbul Kent University, Istanbul, Türkiye, ⁵INPOLDE Research Center, Department of Chemistry, Physics and Environment, Faculty of Sciences and Environment, Dunarea de Jos University of Galati, Galati, Romania, ⁶Computer Engineering Department, Faculty of Engineering and Natural Sciences, Istinye University, Istanbul, Türkiye

Introduction: A lead-acrylic protective screen is suggested to reduce radiation exposure to the unexposed breast during mammography. The presence of toxic lead in its structure may harm the tissues with which it comes in contact. This study aimed to design a CdO-rich quaternary tellurite glass screen (C40) and evaluate its efficiency compared to the Lead-Acrylic protective screen.

Methods: A three-layer advanced heterogeneous breast phantom designed in MCNPX (version 2.7.0) general-purpose Monte Carlo code. Lead acrylic and C40 shielding screens were modeled in the MCNPX and installed between the right and left breast. The reliability of the absorption differences between the lead acrylic and C40 glass were assessed.

Results and discussion: The results showed that C40 protective glass screen has much superior protection properties compared to the lead acrylic protective screen. The amount of total dose absorbed in the unexposed breast for C40 was found to be much less than that for lead-based acrylic. The protection provided by the C40 glass screen is 35–38% superior to that of the Lead-Acrylic screen. The C40 offer the opportunity to avoid the toxic Pb in the structure of Lead-Acrylic material and may be utilized for mammography to offer superior radioprotection to Lead-Acrylic and significantly lower the dose amount in the unexposed breast. It can be concluded that transparent glass screens may be utilized for radiation protection purposes in critical diagnostic radiology applications through mammography.

KEYWORDS

breast dosimetry, mammography, X-ray, radiation protection, MCNPX

1. Introduction

Today, cancer and cancer treatment research are important topics of study for many medical experts (1). Due to its high prevalence and mortality rate among women, breast cancer has a prominent position among the many types of cancers (2). Scientific reports indicate that breast cancer is more manageable if detected at an earlier stage through breast screening programs (3). This is because the most significant tool for early diagnosis is breast screening (4), which is conducted using a variety of systematic methods, including mammography devices (4). Programs for breast cancer screening are a subject that is recognized and addressed in the health policies and public health programs of many countries around the world (5). It is also known that breast screening programs can minimize breast cancer-related mortality rates (6). Utilizing low-energy and ionizing X-rays and mammography equipment, which is important for breast cancer screening programs, is incredibly effective and practical (7). Mammography devices produce low-energy X-rays from the source and guide them onto the breast tissue under investigation. In accordance with the number of absorbed X-rays and X-rays that pass through the breast tissue and reach the image receptor, the patient's anatomic image is generated at the conclusion of the interaction process with the breast tissue. Glandular tissue and possible solid tumors and calcifications may produce X-ray absorption (8) due to their ability to absorb low-energy X-rays. In addition, they may be seen clearly on the collected radiological image as a result of the aforementioned X-ray interaction process (8). This procedure enables the detection of a likely risk factor and, subsequently, the early detection of breast cancer. On the other hand, the use of X-rays for diagnostic procedures should be considered alongside the advantages they bring and the potential negative consequences they represent (9). These risks include DNA mutations (10) generated by the impact of ionizing radiation on biological tissue and radiation-induced breast cancer formations (11). In other words, the mammography technique should be examined holistically, considering its advantages and the reduction in breast cancer mortality rate (12). Fortunately, researchers are extremely motivated to investigate and develop strategies and procedures that help mitigate these risks (13). Numerous international organizations and decision-making authorities, such as the ICRP, have already recommended specific action plans to mitigate these hazards (14, 15). The use of shielding materials and the removal or at least mitigation of unnecessary dose exposure are among the activities that may be performed (16, 17). It is widely known that several organs and tissues in the proximity of this region are also impacted by the dose emitted during breast cancer screening through mammography devices (18, 19). This dose scattering is an inevitable and natural result of the X-ray interaction with the biological tissue just like any material. In this circumstance, the most effective action to take is to prevent and minimize this dose's interaction with neighboring organs and tissues. In addition to the organs and tissues surrounding the exposed breast, the breast in the neighborhood of the exposed breast is also potentially exposed to these backscattered X-rays (18). Because each breast is irradiated two times in the craniocaudal (CC) and mediolateral oblique (MLO) positions during a routine mammography scan (20), the breast that is under examination

is likely exposed to two separate exposures. Several effective investigations on the preservation of breast tissue outside of the extraction region have been conducted by researchers (21, 22). Among them, Koo and Lee (23) evaluated the dose received by the unexamined breast in the neighborhood of the exposed breast by positioning a lead-acrylic transparent protective screen between the two breasts. In their study, a substantial positive impact was found when the protective screen was utilized in terms of radiation protection. They have stressed that the implementation of the protective screen would considerably limit exposure to unnecessary doses. Although the transparency of the lead-acrylic material proposed by Koo and Lee (23) is a crucial factor for the management and monitoring of the other breast during exposure, the presence of toxic lead (24) in its structure may be harmful to the tissues with which it comes in contact. In this study, the protective properties of a cadmium-added glass screen, which may be used as an alternative to the lead-acrylic materials proposed by Koo and Lee (23), were examined and compared in terms of the same sizes and geometric properties. The acquired results might give crucial information for the development of protective screens, which can be an effective way of protecting radiosensitive organs and minimizing the prevalence of secondary malignancies caused by unnecessary exposure. In addition, given that glass materials are an important family of materials used in radiation protection (25) and that the literature has been intensively studied over the past few years (26–28), it is expected that the results would therefore make significant contributions to the literature of glasses that can be used for radiation protection.

2. Materials and methods

In the first phase, a basic phantom design was developed, which included the right and left breast, body phantom, and X-ray source. In the second phase of the investigation, standard data were used to evaluate the phantom's reliability. In the third and final phase, a separate design was constructed, which included the installation of a shielding screen between the right and left breasts. In this section, technical details about these three phases are presented.

2.1. Modeling and simulation details

The physical construction and all modeling steps of the breast phantom used in the investigation were accomplished using version 2.7.0 of MCNPX (29), a well-known and general-purpose Monte Carlo tool. Eventually, a breast phantom with three layers was generated. A unique Glandular Fraction value was given to each layer in the left and right breasts. This three-layer heterogeneous breast model has recently been proposed by Chang et al. (30) for advanced breast dosimetry studies. Figure 1 shows the 2D view of modeled breasts along with the body phantom from (a) the top and (b) the side view. The glandular fraction (GF) coefficients of the modeled layers were derived in line with a previously studied geometric principle. Each layer was designated as a unique CELL inside the MCNPX input file. The contents of these CELL volumes, as well as their elemental percentage fractions and densities, were

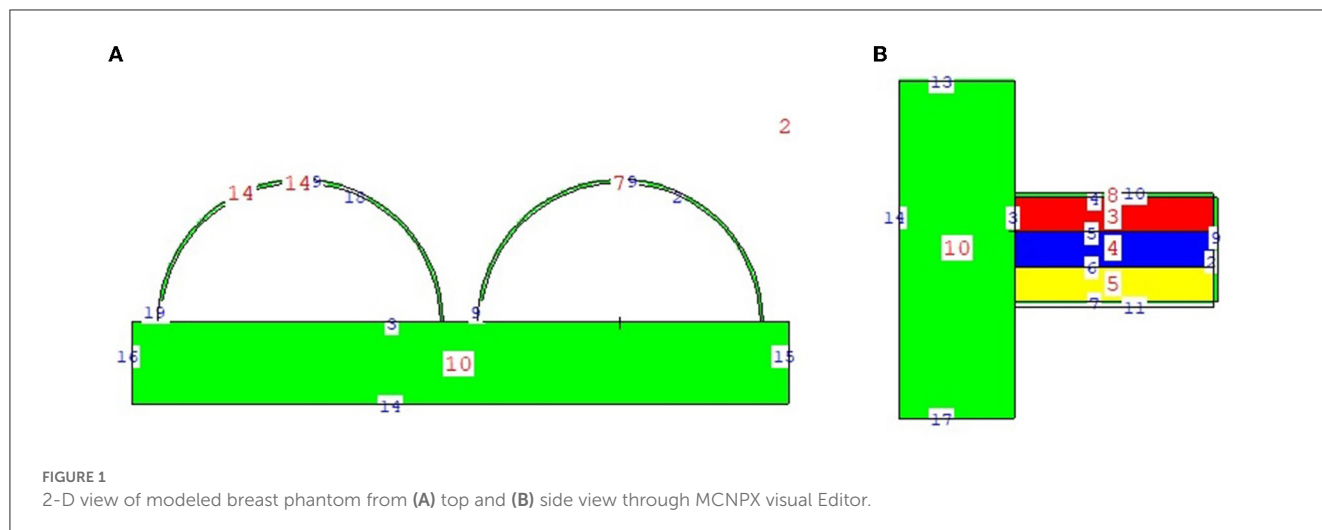


TABLE 1 Elemental properties and densities of the modeled breast layers (30).

Tissue	Density (g/cm ³)	Weight percentage (%)			
		H	C	N	O
GF tissue (25%)	0.955	11	51	2.1	35.7
GF tissue (50%)	0.982	10.7	40.1	2.5	46.4
GF tissue (75%)	1.010	10.5	29.3	2.9	57
Skin	1.090	9.8	17.8	5	66.7

provided in the INPUT file in accordance with the different GF values. In addition to their constituent percentages and densities (see Table 1), the skin layers around the five surfaces of the three-layer breast model were also specified for the left and right breasts. On the back of the generated breast model, a human-tissue-dense body phantom was incorporated toward the input. In the final stage, a breast phantom-specific source with a source-image receptor distance of 65 cm was designed. Figures 2, 3 show the 3D view of the modeled breasts from the top and the side view. Figure 2 demonstrates that a 2-mm skin layer was placed on both breasts. Moreover, the X-ray source was placed over the right breast. The first is the primary layer with which the primary X-rays will interact based on the direction of their entrance. X-rays that pass through the first layer will correspondingly penetrate the second and third levels. These layers' absorption will decrease the number of X-rays that reach the image detector. Figure 3 depicts, from the side, the sequence of layers in the modeled breast phantom based on the location of the X-ray source.

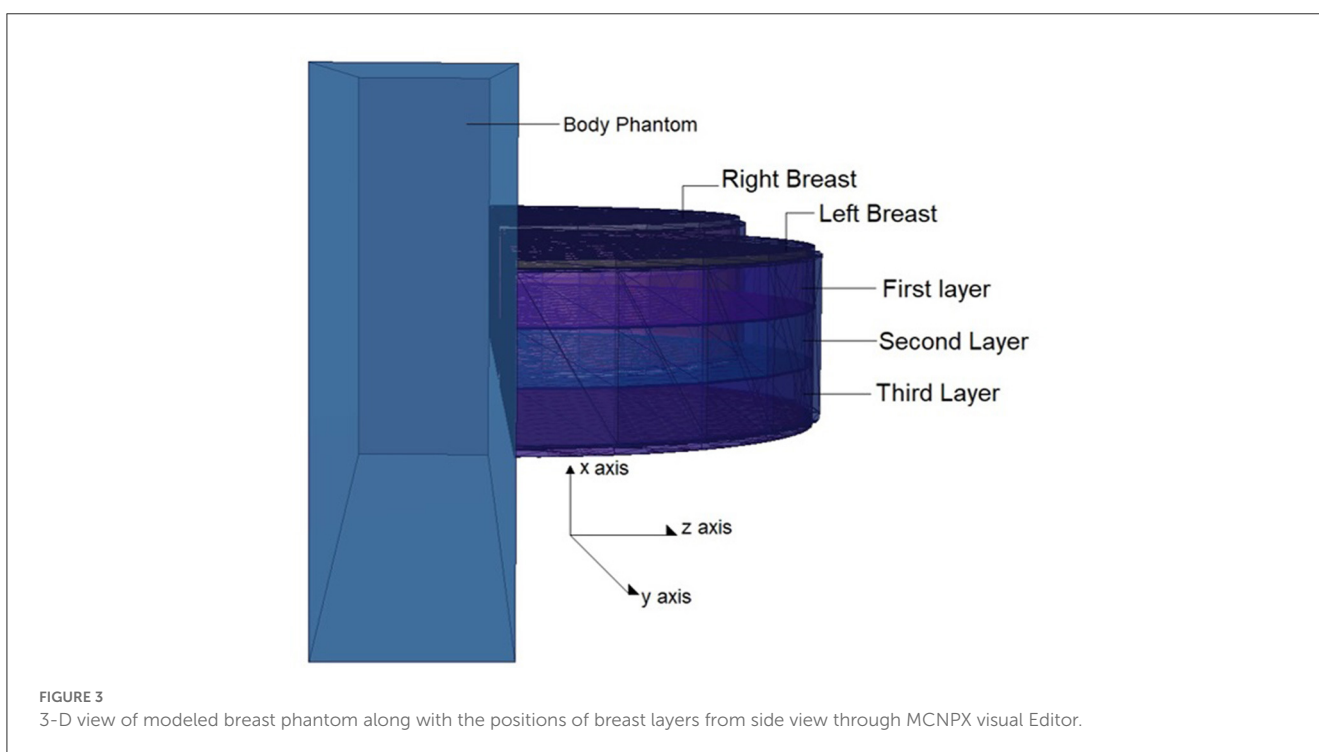
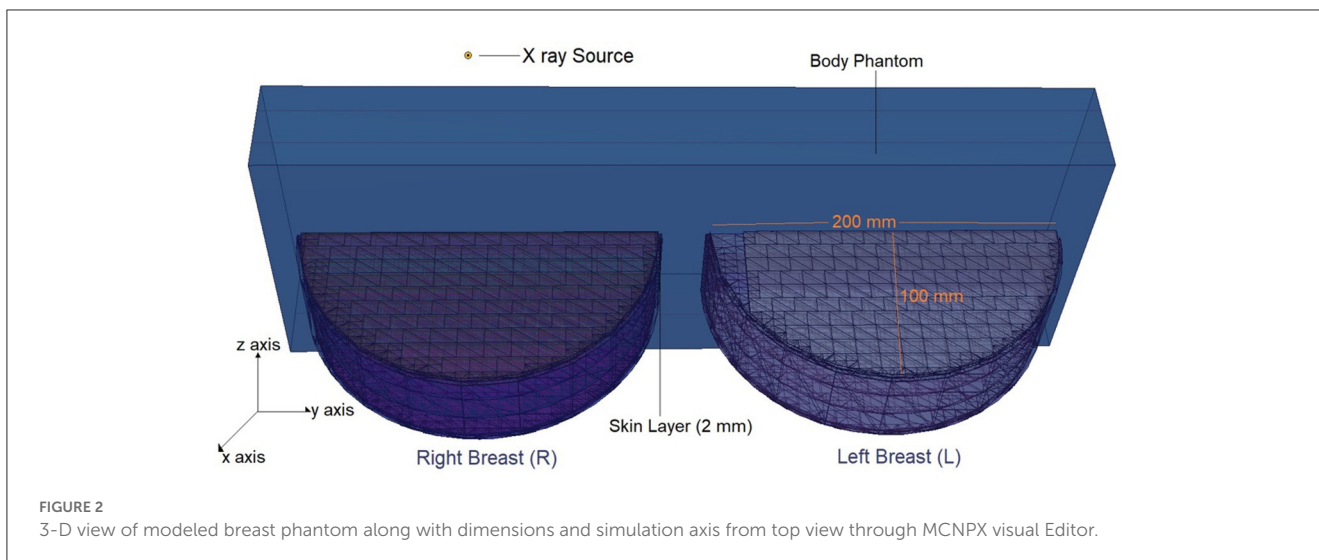
2.2. Validation of MCNPX

In the first step of the investigation, the MCNPX code verification procedure was conducted. This verification process was conducted in accordance with the dosimetry guideline for mammographic techniques detailed in the AAPM TG-195 (31)

report. Using the report's specified parameters and dimensions, a breast phantom with an adipose-to-glandular tissue ratio of 80 to 20% was modeled. More technical information on the breast phantom model may be found in the resource handbook (31). Using the F6 Tally Mesh, a major tally variation of the MCNPX algorithm, the quantity of energy deposited per unit volume is then computed. Based on three iterations, this procedure yielded a result of 4,782 eV/photon (4,782 eV energy transferring per photon). Compared to the data in the source guide, a discrepancy of 3% was found. This variance is within acceptable limits, and it is believed that it is attributable to computer hardware, processor, and other simulation features. Once verification was accomplished, the next steps of the investigation were carried out.

2.3. Modeling of lead-acrylic and C40 shielding screen

Following the basic modeling outlined earlier, a second input code file was created. The difference in this second input code was the shielding screen that was placed between the right and left breasts, and the input file included both surface and cellular definitions of the modeled screen using elemental mass fractions (wt.%) and material density (g/cm³). The dimensions of the modeled shielding screen are defined as 20 × 20 cm². In later phases of the study, the structure of the material in the input file was defined separately as lead-acrylic (23) and C40 cadmium oxide-rich glass. This was done to analyze the absorption differences between the lead-acrylic and C40 glass (32) screens, which was also the primary purpose of the study, and to determine how much it decreased the dose delivered to the unexposed breast. It is worth mentioning that the C40 glass screen was synthesized by the research team (32) as a CdO (cadmium oxide)-rich quaternary tellurite glass for nuclear safety purposes. In a previous study (23), it was found that the absorption equivalent of a 12-mm thick lead-acrylic material is comparable to that of a 0.5-mm thick lead (Pb). In the reference study (23), lead acrylic is recommended as a shielding screen with dimensions of 20 × 20 cm² and a thickness of 12 mm. Consequently, the proposed lead acrylic with

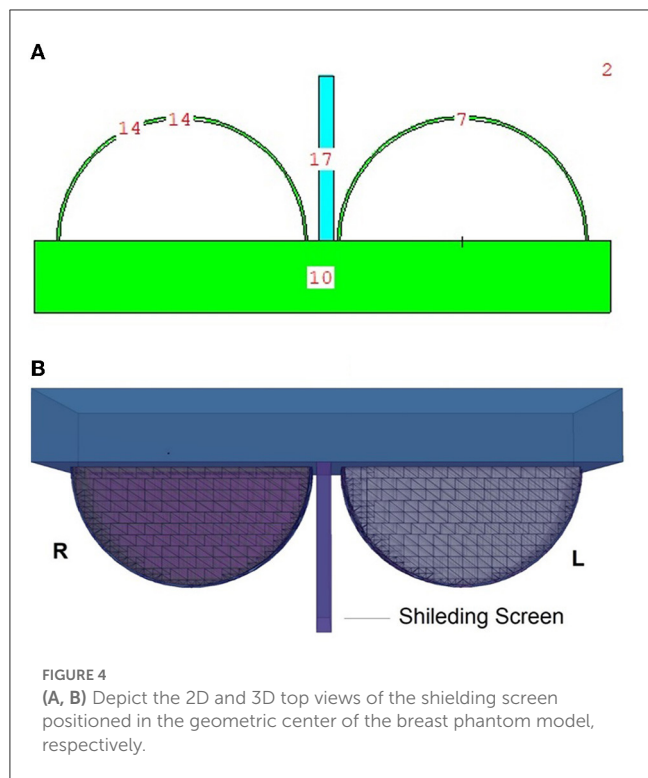


the same dimensions was modeled in the MCNPX and inserted between the right and left breasts. Next, the same dimensions were used for the design of the C40 shielding screen as well. Using the specific properties, such as elemental mass fractions (wt. %) and density (g/cm^3), for C40 glass, the cellular structure line was modified in the input file, yet the geometric dimensions in the surface cards remained unchanged. This enabled us to examine the absorption properties of C40 transparent glass, which has the same dimensions and thickness as the specified lead acrylic, with dimensions of $20 \times 20\text{ cm}^2$ and a thickness of 12 mm. The center of the shielding screen was determined as the geometric center of the left and right breasts. Figure 4 depicts the 2D and 3D top views of the shielding screen positioned in the geometric center of the breast phantom model. Meanwhile, the C40 sample, which is

rich in cadmium oxide, was manufactured by our team and was suggested in previous studies as a promising material in terms of its transparency and radiation-absorbing properties. The primary objective of this research was to investigate the applicability of C40 material for medical procedures, considering its transparency and exceptional radiation absorption qualities.

3. Results and discussion

In this study, the reduction in the amount of dose absorbed in the non-exposed breast compared to the exposed breast caused by the mammography device used in routine breast screening procedures was investigated. A fully-fledged breast phantom

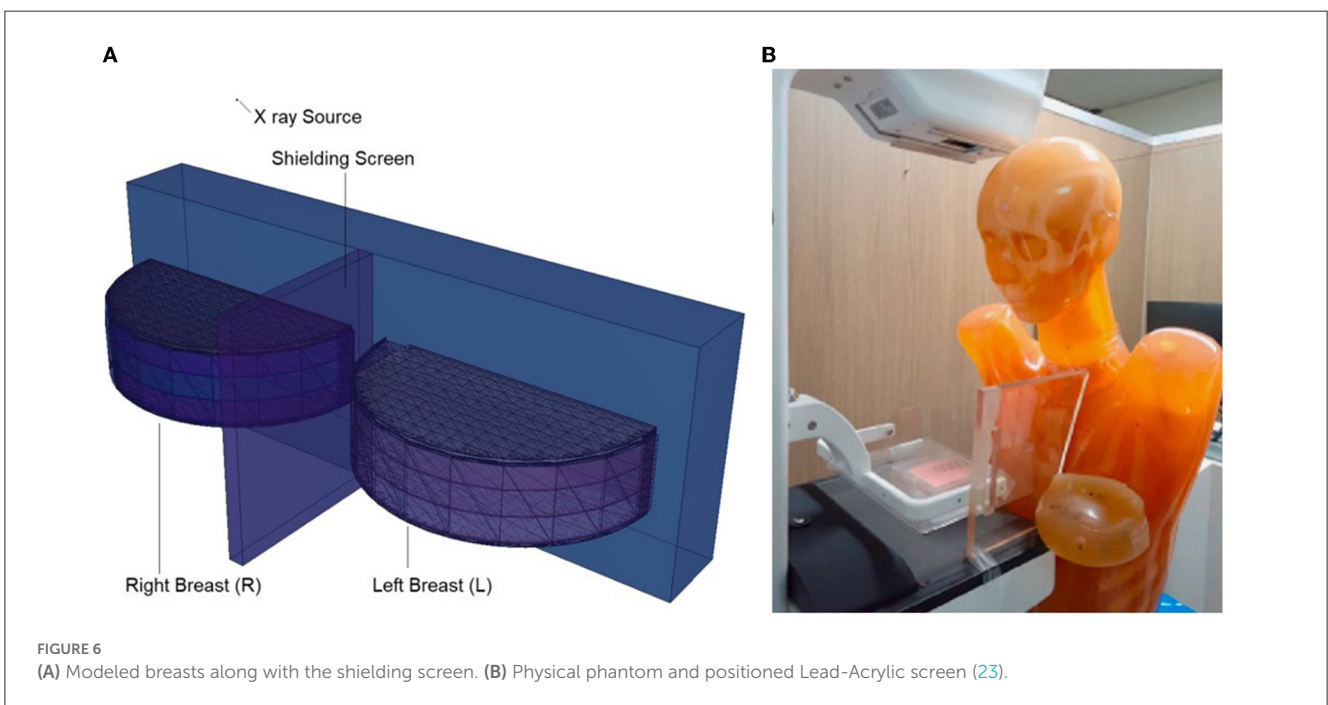
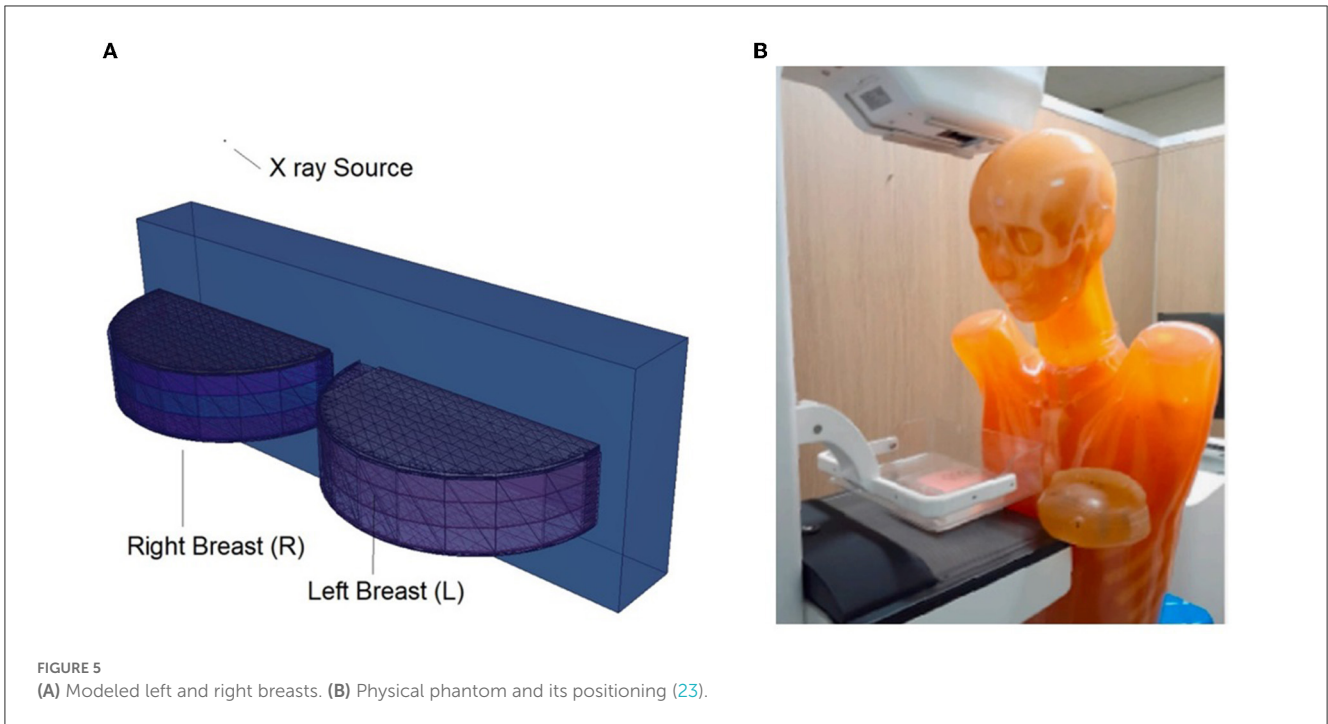


design, as indicated by international publications, was developed for the investigation. In a previous study published (23) in the scientific literature, the dose to the non-exposed breast was lowered using a lead-acrylic protection screen, and substantial results were observed. In this study, the experimental phantom was designed with all its geometrical characteristics and positioning, and the suggested protective C40 transparent glass screen for the unexposed left breast was thoroughly compared with the experimental data obtained through a lead-acrylic protection screen. In the first phase of the study's results, the experimental phantom shown in Figure 5B was designed in MCNPX. Although a uniform breast phantom was employed in the experimental investigation, a three-layer advanced heterogeneous breast phantom (see Figure 5A) was used in this study to raise the degree of coverage of the results for each modeled breast layer. This allowed the researchers to study the protective characteristics of the protective screen on a layer-by-layer basis and make more specific recommendations as a function of the modeled breast layers from the first to third breast layers, respectively. Figure 6B depicts the positioning of the lead-acrylic protective screen utilized in the experimental investigation between the two breasts, as well as the condition of the left breast and the positioning of the lead-acrylic protective screen during exposure to the right breast. This experimental setup was constructed similarly in MCNPX Monte Carlo code seen in Figure 6A, and the protective screen was positioned between two breast structures with equal experimental dimensions. Meanwhile, prior to breast dosimetry investigations, the transmission factors (TF) of the compared protective screens were determined. TF is the mathematical ratio between the intensity of the initial photon encountered on one side of a material and the intensity remaining on the other side of the material. These

values are physical characteristics that provide crucial information about the material's absorption capacity, and they are recognized as an absorption parameter utilized in numerous investigations. Prior to examining the radiation shielding properties provided by the two compared shielding materials, the primary objective of this pilot study was to obtain some different comparison results that would validate the absorption properties to be obtained in the subsequent phases by observing the percentage reductions in the photon intensity at specific energies. For this initial phase, two detection zones in front of and behind the absorber material were constructed. As the main gamma-ray intensity, photons generated by an isotropic point source were evaluated. After interacting with the absorber material, photons that were counted as the secondary photon amount on the material's backside were also tallied in the detection region behind the absorber material. Figure 7 depicts the TF values and the rate of change of these values from a lead-acrylic screen to a C40 glass screen by calculating the ratios of the secondary photon quantity to the primary photon quantity. As demonstrated in Figure 7, the number of primary photons was seen to be the same in both situations. This is an anticipated result of using the same energy value as the source. However, the values of secondary photons were different, with a lower value for C40. This decrease in the number of secondary photons observed for C40 was reflected in the proportionality value resulting in a lower TF for C40 (see Equation 1).

$$\text{Transmission Factor (TF)} = \frac{\text{Photon Flux}_{\text{Secondary}}}{\text{Photon Flux}_{\text{Primary}}} \quad (1)$$

In the second phase of the investigation, the total skin layer dose in the right and left breasts was determined for instances involving the use of lead acrylic and C40. Figure 1B depicts the 2 mm skin layer surrounding the breast as seen from the side. As shown in Figure 1B, cells 9, 10, and 11 represent independently modeled skin layers, and the output values for these cells were acquired and summed separately. This sum was taken into consideration as the overall skin dose per irradiation. Figure 8 shows the variations in the total skin dose per irradiation when lead acrylic and C40 were utilized. As shown in Figure 9, the dose of the right breast did not vary for each energy value in either material. However, owing to the increase in energy, the ratio of total skin dosage in the right breast increased. For a given energy value, the dose to the unexposed left breast varied according to the use cases of lead acrylic and C40. If the unexposed left breast was shielded by a C40 protective monitor, the total skin dose calculated by three different cells for the left breast was far less for each energy value. This demonstrates that the quantity of dose received by the whole skin layer around the breast will be reduced when a C40 protective monitor is used as compared to a lead-acrylic monitor. Previous research (23) has shown that the lead-acrylic protective screen decreases the skin dose. This condition demonstrates that if the unexposed breast is shielded by an absorbent material, the skin dose, which also affects the glandular dose, would decrease, and this is seen as a crucial step in protecting the tissues around the examination area. This study's primary purpose was to demonstrate the potential differences between the transparent C40 protective glass screen and the lead-acrylic protective screen. In accordance



with the objective, it has been found, based on TF and total skin dose values, that the C40 protective glass screen has superior protection properties compared to the lead-acrylic material and may be utilized to further reduce the total skin dose of the unexposed breast during the routine mammography examinations. In the third phase of the study, following the total skin dose reduction, the absorbed dose amounts for three different breast phantom layers were independently evaluated and compared. Figure 10 depicts the unexposed and shielded left breast dose as a

function of increasing energy for the three modeled layers. As seen in the figure, the maximum dose is counted in the first layer for both lead acrylic and C40. The reason for this could be explained by the proximity of these three breast model layers to the X-ray source. As shown in Figure 3, layer 1 is the uppermost layer and the area that is geometrically closest to the X-ray source. In accordance with the ALARA principle, as the distance from the source increases, the exposure rate decreases in accordance with the inverse square law. This is also obvious from the difference

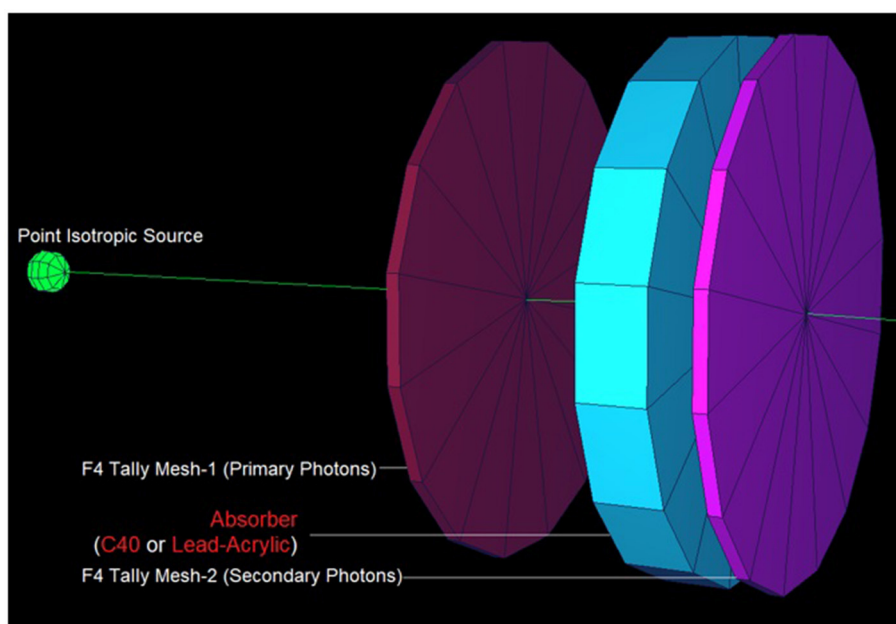


FIGURE 7
Designed MCNPX simulation setup for TF calculations for C40 and Lead-Acrylic protection screens.

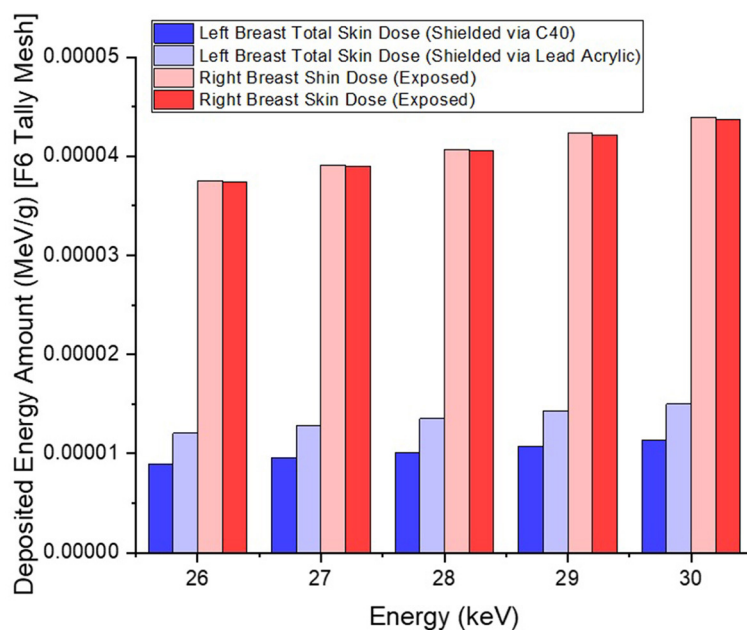


FIGURE 8
Variation of total skin doses for left and right breasts.

between the total dose received by the first and second breast layers. The second and third breast layers, which are further away from the X-ray source than the first, were subjected to a lower dose. This is a significant result that may imply that greater emphasis should be placed on locations closer to the X-ray source during the protection of the unexposed breast during mammography. When C40 was utilized, however, the absorbed dose amounts in each of

the three layers were seen to be lower. This is accurate for all three layers and is a key signal showing the overall superiority of C40 in protecting the breast that is not exposed and should be protected. Using the overall dose amounts as a sum of the three layers, the results for the three layers have been verified. Figures 11, 12 show the fluctuation of the total dose absorbed in the right and left breasts as a function of energy when lead acrylic and C40 are used as

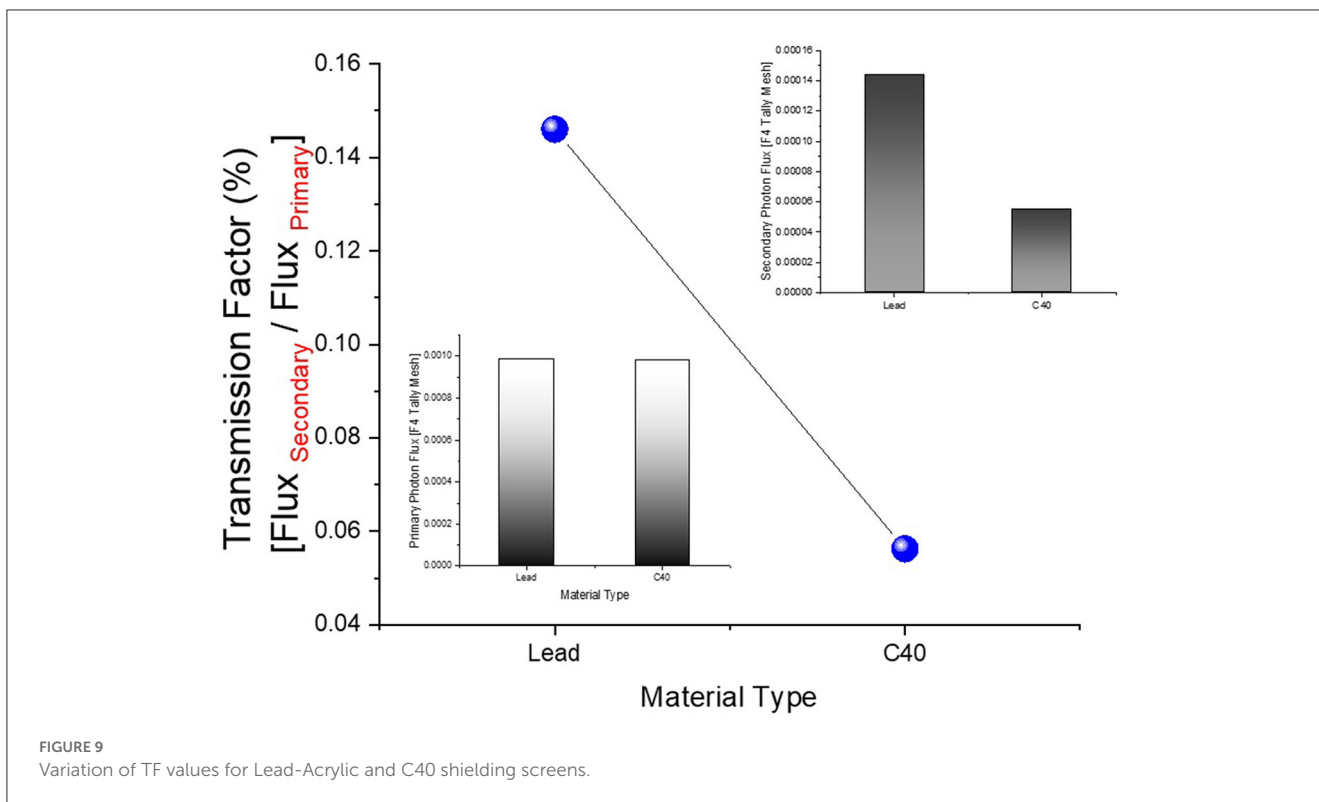


FIGURE 9 Variation of TF values for Lead-Acrylic and C40 shielding screens.

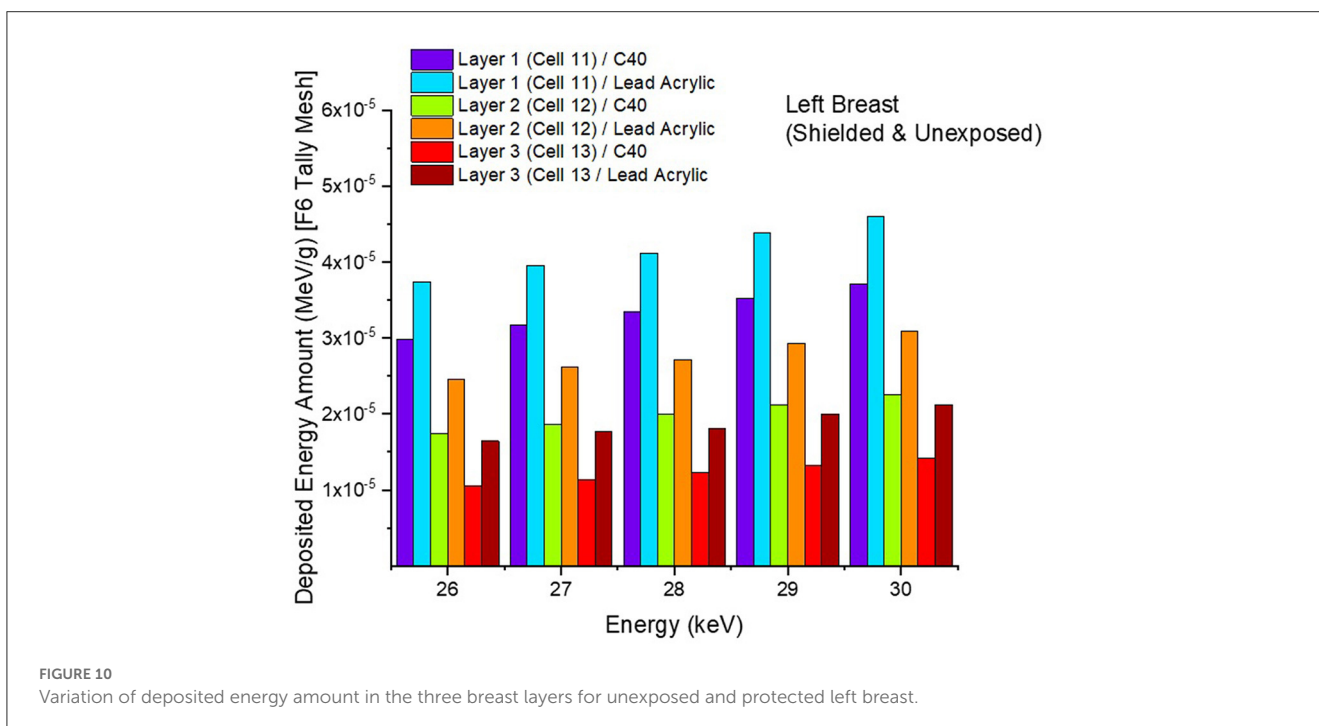


FIGURE 10 Variation of deposited energy amount in the three breast layers for unexposed and protected left breast.

protective screens. As seen in Figure 11, the total dose received by the exposed right breast increased as the energy level increased. While dose ratios for the right breast did not have an important impact in the study, the purpose of this outcome is to emphasize the importance of using X-rays in the mammography technique

and to illustrate that the protective screen used has no impact on the exposed breast. The minor differences seen in Figure 11 are attributable to the technical variations inherent to the Monte Carlo simulation. Figure 12 depicts the deposited energy amount in the unexposed and shielded left breast as the sum of the measured doses

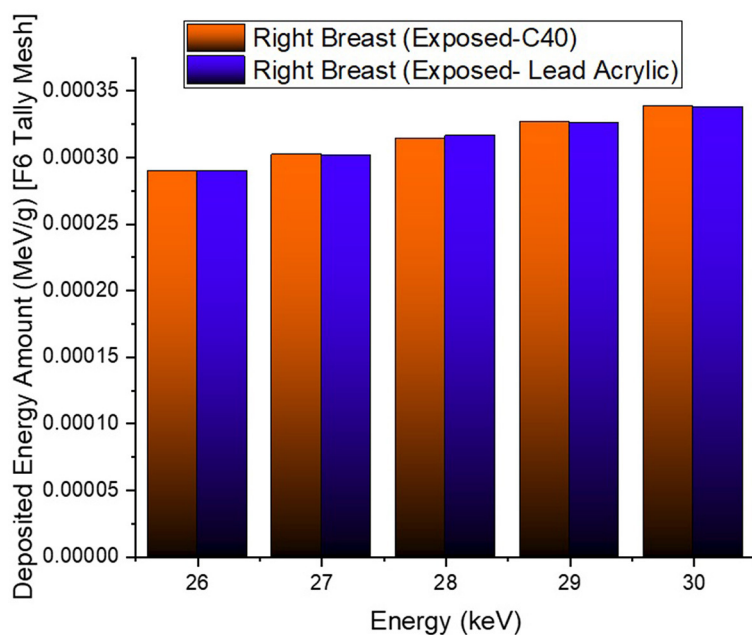


FIGURE 11
Variation of total deposited energy amount in the right breast.

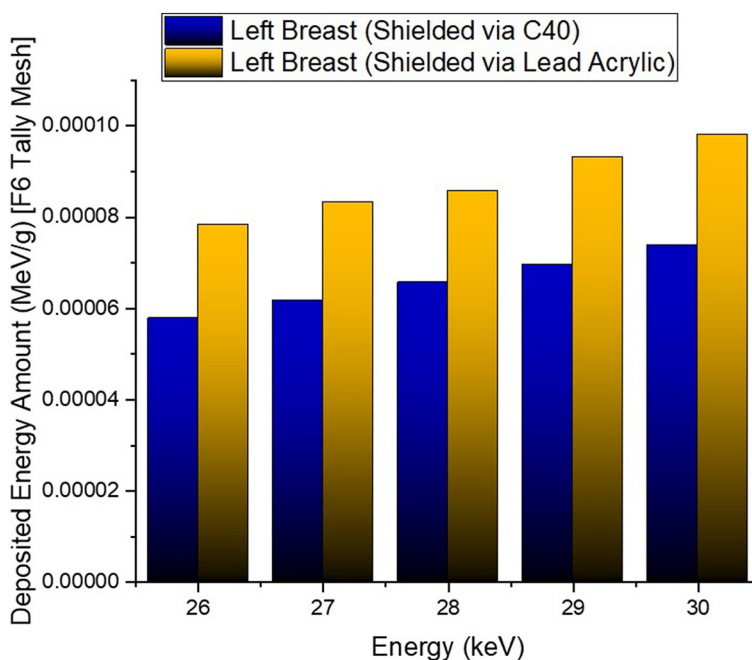


FIGURE 12
Variation of total deposited energy amount in the left breast.

in the three layers for different X-ray energies. Even though the dose values absorbed in different breast layers vary as a function of distance from the source, the total dose absorbed in the left breast for C40 was found to be much less than that for lead-based acrylic. This change is reported to lead to improved protective properties for C40, with a difference of 35–38% for all energy levels.

4. Conclusion

Mammography, an X-ray-based diagnostic method, is the most critical phase in breast cancer screening programs. This is the standard procedure for screening programs for women over a certain age. This procedure might result in routine dose exposure

as part of the diagnostic process, but it provides considerable health advantages. The objective of this research was to assess the radiation protection properties of a CdO-added glass screen (C40) by introducing a unique dose reduction strategy for mammography operations. Considering a previous clinical investigation, the C40 screen was designed with the same geometric proportions. The acquired outcomes were compared to the lead-acrylic material that was evaluated in the reference experimental study. The results indicate that the C40 glass screen is 35–38% more protective than the lead-acrylic screen. Considering the drawbacks of lead-hazardous acrylic's Pb structure, it can be concluded that glasses rich in cadmium oxide may be employed in mammography procedures since they provide better radioprotection than lead-acrylic and significantly reduce the dose amount in the unexposed left breast. This decrease will not only reduce the risk of breast cancer from radiation exposure but may also reduce radiation-induced cancer types. It can be concluded that the C40 protective screen would contribute to clinical applications as a shielding material for unexposed breasts due to its transparency in the visible light spectrum, ease of manufacture, and outstanding properties as a glass material. Many women have a mammogram every year. Nonetheless, there is a significant need for healthcare systems to focus on delivering high-quality services, with a strong emphasis on the patient experience. Therefore, protecting the unexposed breast is a wonderful way of spreading awareness of the importance of preventing unnecessary radiation exposure while providing the required medical care. On the other hand, based on the findings from this investigation, it has been demonstrated once again that Monte Carlo simulation-based radiation transport processes are an essential tool for medical radiation research. Particularly in studies concentrating on concept design, the implementation of extensive simulation techniques at this stage may serve as a crucial motivation for material manufacturing and the industrial phase. This research only examined exposed and unexposed breast tissues. In future studies, the current phantom might be expanded and examined for organs that are likely to suffer harm due to mammography procedures, including the brain, thyroid, heart, and lungs.

Data availability statement

The raw data supporting the conclusions of this article will be made available by the authors, without undue reservation.

References

- dos Santos AF, De Almeida DRQ, Terra LF, Baptista MS, Labriola L. Photodynamic therapy in cancer treatment—an update review. *J Cancer Metast Treat.* (2019) 5:25. doi: 10.20517/2394-4722.2018.83
- Azamjah N, Soltan-Zadeh Y, Zayeri F. Global trend of breast cancer mortality rate: a 25-year study. *Asian Pacific J Cancer Prevent.* (2019) 20:2015. doi: 10.31557/APJCP.2019.20.7.2015
- Homan SG, Yun S, Bouras A, Schmaltz C, Gwanfogbe P, Lucht J. Breast cancer population screening program results in early detection and reduced treatment and health care costs for Medicaid. *J Public Health Manage Pract.* (2021) 27:70–9. doi: 10.1097/PHH.0000000000001041
- Duffy SW, Tabár L, Yen AMF, Dean PB, Smith RA, Jonsson H, et al. Mammography screening reduces rates of advanced and fatal breast cancers: Results in 549,091 women. *Cancer.* (2020) 126:2971–9. doi: 10.1002/cncr.32859
- Dibden A, Offman J, Duffy SW, Gabe R. Worldwide review and meta-analysis of cohort studies measuring the effect of mammography screening programmes on incidence-based breast cancer mortality. *Cancers.* (2020) 12:976. doi: 10.3390/cancers12040976
- Katalinic A, Eisemann N, Kraywinkel K, Nofzt MR, Hübner J. Breast cancer incidence and mortality before and after implementation

Author contributions

GA: writing, simulations, and investigation. WE: writing and investigation. ER: writing, investigation, and data curation. GK, EI, and DS: investigation and data curation. AE: funding acquisition, investigation, and data curation. HT: writing, simulations, investigation, and supervision. All authors contributed to the article and approved the submitted version.

Funding

The funding was provided by the Princess Nourah Bint Abdulrahman University Researchers Supporting Project number (PNURSP2023R149), Princess Nourah Bint Abdulrahman University, Riyadh, Saudi Arabia.

Acknowledgments

The authors would like to express their deepest gratitude to Princess Nourah Bint Abdulrahman University Researchers Supporting Project number (PNURSP2023R149), Princess Nourah Bint Abdulrahman University, Riyadh, Saudi Arabia. AE acknowledges the material support of the Dunarea de Jos University of Galati.

Conflict of interest

The authors declare that the research was conducted in the absence of any commercial or financial relationships that could be construed as a potential conflict of interest.

Publisher's note

All claims expressed in this article are solely those of the authors and do not necessarily represent those of their affiliated organizations, or those of the publisher, the editors and the reviewers. Any product that may be evaluated in this article, or claim that may be made by its manufacturer, is not guaranteed or endorsed by the publisher.

- of the German mammography screening program. *Int J cancer*. (2020) 147:709–18. doi: 10.1002/ijc.32767
7. Heyes GJ, Mill AJ, Charles MW. Mammography—Oncogenicity at low doses. *J Radiol Protect*. (2009) 29:123. doi: 10.1088/0952-4746/29/2A/S08
8. Bushong SC. *Radiologic Science for Technologists E-Book: Physics, Biology, and Protection*. St. Louis: Elsevier Health Sciences. (2020).
9. Šalát D, Nikodemová D, Klepanec A, Lehotská V, Šalátová A. Diagnostic reference levels in screening mammography centers in Slovakia. *Radiat Prot Dosimetry*. (2022) 198:537–9. doi: 10.1093/rpd/ncac095
10. Borrego-Soto G, Ortiz-López R, Rojas-Martínez A. Ionizing radiation-induced DNA injury and damage detection in patients with breast cancer. *Genet Mol Biol*. (2015) 38:420–32. doi: 10.1590/S1415-475738420150019
11. Golubicic I, Borojevic N, Pavlovic T. Risk factors for breast cancer is ionizing radiation among them. *J Buon*. (2008) 13:487–94.
12. Brown M, Covington MF. Comparative benefit-to-radiation risk ratio of molecular breast imaging, two-dimensional full-field digital mammography with and without tomosynthesis, and synthetic mammography with tomosynthesis. *Radiol Imaging Cancer*. (2019) 1:e190005. doi: 10.1148/rycan.2019.90005
13. Fishman MD, Rehani MM. Monochromatic X-rays: The future of breast imaging. *Eur J Radiol*. (2021) 144:109961. doi: 10.1016/j.ejrad.2021.109961
14. Hendrick RE. Radiation doses and cancer risks from breast imaging studies. *Radiology*. (2010) 257:246–53. doi: 10.1148/radiol.10100570
15. Vaňo E, Miller DL, Martin CJ, Rehani MM, Kang K, Rosenstein M, et al. ICRP publication 135: diagnostic reference levels in medical imaging. *Ann ICRP*. (2017) 46:1–144. doi: 10.1177/0146645317717209
16. Elshami W, Abuzaid MM, Tekin HO. Effectiveness of breast and eye shielding during cervical spine radiography: an experimental study. *Risk Manag Healthc Policy*. (2020) 13:697. doi: 10.2147/RMHP.S257185
17. Elshami W, Tekin HO, Issa SA, Abuzaid MM, Zakaly HM, Issa B, et al. Impact of eye and breast shielding on organ doses during cervical spine radiography: design and validation of MIRD computational phantom. *Front Public Health*. (2021) 9:751577. doi: 10.3389/fpubh.2021.751577
18. Ali RM, England A, Mercer C, Tootell A, Walton L, Schaake W, et al. Mathematical modelling of radiation-induced cancer risk from breast screening by mammography. *Eur J Radiol*. (2017) 96:98–103. doi: 10.1016/j.ejrad.2017.10.003
19. Ali RMKM. *Risk of Radiation-Induced Cancer From Screening Mammography*. United Kingdom: University of Salford. (2016).
20. Popli MB, Teotia R, Narang M, Krishna H. Breast positioning during mammography: mistakes to be avoided. *Breast Cancer*. (2014) 8:17617. doi: 10.4137/BCBCR.S17617
21. Ali RM, England A, Mercer CE, Tootell AK, Hogg P. Impact of contralateral breast shielding on the risk of developing radiation-induced cancer from full-field digital mammography screening. *J Med Imag Radiat Sci*. (2019) 50:331–6. doi: 10.1016/j.jmir.2019.02.005
22. Pyka M, Eschle P, Sommer C, Weyland MS, Kubik R, Scheidegger S. Effect of thyroid shielding during mammography: measurements on phantom and patient as well as estimation with Monte Carlo simulation. *Eur Radiol Exper*. (2018) 2:1–10. doi: 10.1186/s41747-018-0042-9
23. Koo BY, Lee KS. Reduction of scattered radiation dose by X-ray shielding during mammography. *Radiat Phys Chem*. (2020) 177:109111. doi: 10.1016/j.radphyschem.2020.109111
24. Ara A, Usmani JA. Lead toxicity: a review. *Interdiscip Toxicol*. (2015) 8:55. doi: 10.1515/intox-2015-0009
25. Tekin HO, ALMisned G, Rammah YS, Ahmed EM, Ali FT, Baykal DS, et al. Transmission factors, mechanical, and gamma ray attenuation properties of barium-phosphate-tungsten glasses: Incorporation impact of WO₃. *Optik*. (2022) 267:169643. doi: 10.1016/j.ijleo.2022.169643
26. Tekin HO, ALMisned G, Rammah YS, Susoy G, Ali FT, Baykal DS, et al. The significant role of WO₃ on high-dense BaO–P₂O₃ glasses: transmission factors and a comparative investigation using commercial and other types of shields. *Appl Phys A*. (2022) 128:1–11. doi: 10.1007/s00339-022-05620-y
27. Tekin HO, Ali FT, Almisned G, Susoy G, Issa SA, Ene A, et al. Multiple assessments on the gamma-ray protection properties of niobium-doped borotellurite glasses: A wide range investigation using Monte Carlo simulations. *Sci Technol Nucl Install*. (2022) 2022. doi: 10.1155/2022/5890896
28. Zakaly HM, Tekin HO, Rammah YS, Issa SA, Alomari AH, Ali FT, et al. Physical features of high-density barium–tungstate–phosphate (BTP) glasses: elastic moduli, and gamma transmission factors. *Electronics*. (2022) 11:4095. doi: 10.3390/electronics11244095
29. RSICC Computer Code Collection. *MCNPX user's manual version 2.4.0. Monte Carlo N-Particle Transport Code System for Multiple and High Energy Applications* (2002).
30. Chang TY, Lai KJ, Tu CY, Wu J. Three-layer heterogeneous mammographic phantoms for Monte Carlo simulation of normalized glandular dose coefficients in mammography. *Sci Rep*. (2020) 10:2234. doi: 10.1038/s41598-020-59317-4
31. Sechopoulos I, Ali ES, Badal A, Badano A, Boone JM, Kyprianou IS, et al. Monte Carlo reference data sets for imaging research: Executive summary of the report of AAPM Research Committee Task Group 195. *Med Phys*. (2015) 42:5679–91. doi: 10.1118/1.4928676
32. Kilic GÖ, Kavaz E, Ilik ER, ALMisned G, Tekin HO. CdO-rich quaternary tellurite glasses for nuclear safety purposes: Synthesis and experimental gamma-ray and neutron radiation assessment of high-density and transparent samples. *Optical Mater*. (2022) 129:112512. doi: 10.1016/j.optmat.2022.112512